Uptake of ^{18}F-FDG in Acute Aortic Dissection: A Determinant of Unfavorable Outcome

Kimihiko Kato[1], Akiko Nishio[2], Noriyuki Kato[3], Hisashi Usami[2], Tetsuo Fujimaki[1], and Toyoaki Murohara[4]

[1]Department of Cardiovascular Medicine, Gifu Prefectural Tajimi Hospital, Tajimi, Japan; [2]Department of Radiology, Nagoya University, Graduate School of Medicine, Nagoya, Japan; [3]Department of Radiology, Mie University, Graduate School of Medicine, Tsu, Japan; and [4]Department of Cardiology, Nagoya University Graduate School of Medicine, Nagoya, Japan

Imaging with ^{18}F-FDG PET/CT is able to reveal vascular inflammation, and several studies have shown that increased ^{18}F-FDG uptake in carotid artery plaques can qualify the degree of atherosclerotic inflammation. However, clinical assessment of acute aortic dissection (AAD) by PET/CT remains largely unexplored. This study aimed to investigate the use of ^{18}F-FDG PET/CT to predict short- and midterm outcomes in medically controlled AAD patients. **Methods:** A total of 28 medically treated AAD patients (2 Stanford type A and 26 type B, aged 69.5 ± 11.6 y) were prospectively studied. All patients were examined by enhanced CT for diagnosis of AAD and underwent serial imaging studies during follow-up. PET/CT images were acquired 50 and 100 min after ^{18}F-FDG injection in all patients in the acute phase. **Results:** Of the 28 patients, 8 who had an unfavorable outcome due to death from rupture ($n = 2$), surgical repair ($n = 4$), and progression of dissection ($n = 2$) were categorized as having unfavorable AAD. The remaining 20 patients were categorized as having favorable AAD. Maximum dissection diameter in the unfavorable group was significantly greater than that in the favorable group ($P = 0.0207$). On 50-min images, maximal and mean standardized uptake values (SUVs) at maximum aortic dissection sites were significantly greater for the unfavorable group than for the favorable group (all $P < 0.01$). A stepwise-forward selection procedure demonstrated that the mean SUV at sites of maximum aortic dissection on 50-min images significantly and independently predicted an unfavorable outcome for AAD ($P = 0.0171$; odds ratio, 7.72; 95% confidence interval, 1.44–41.4; $R^2 = 0.2372$). A mean SUV greater than 3.029 had significant predictive power, with sensitivity of 75.0%, specificity of 70.0%, a positive predictive value of 50.0%, a negative predictive value of 87.5%, and accuracy of 71.4%. **Conclusion:** Greater uptake of ^{18}F-FDG in AAD was significantly associated with an increased risk for rupture and progression. ^{18}F-FDG PET/CT may be used to improve AAD patient management, although more studies are still needed to clarify its role in this clinical scenario.

Acute aortic dissection (AAD) is a life-threatening condition that arises from an atherosclerotic lesion in the aorta and is a leading cause of mortality (1). Current outcomes of medical therapy for Stanford type B AAD remain poor, with early mortality ranging from 10% to 12% (2,3). Medical management for AAD, particularly for Stanford type B, poses the difficult problem of deciding on whether surgery is needed and when it should be performed. The decision should balance the surgical risk and the hazard of aortic rupture in elective cases of Stanford type B AAD and in the elderly (4). Close, long-term CT monitoring of morphologic parameters, including maximum aortic diameter and the shape of the dissection, is helpful both for preventing aortic rupture and for undertaking timely surgical or endovascular intervention (5). However, only the relative and not the individual risk of rupture can be determined (6). Hence, we need to better understand the factors leading to progression and rupture of AAD in patients on conservative medical therapy. A better understanding may lead to better selection of those patients at higher risk of rupture, who can then be switched to surgical therapy.

Aortic dissection has been defined as separation of the aortic wall layers (4). Stanford type A AAD involves the ascending aorta or aortic arch, progressing distally toward the descending thoracic aorta, and type B AAD occurs distal to the left subclavian artery (7). Dissecting aneurysms of the thoracic aorta develop as a result of progressive weakening of the aortic wall. In current pathologic perspectives, metabolic processes including chronic inflammation and proteolysis play a crucial role in degeneration of the aortic wall, resulting in the formation, progression, and rupture of AAD (8,9).

There is growing evidence, with histologic validation, that increased ^{18}F-FDG uptake constitutes a potential marker of active atherosclerotic inflammation within the aorta and the carotid, iliac, femoral, and vertebral arteries (10–12). With the glucose analog ^{18}F-FDG, PET can acquire images of vascular inflammation, primarily because of increased macrophage metabolism (13). However, PET is limited by its inability to precisely localize the site of increased tracer uptake. Combined PET/CT using the same imaging device allows for correct fusion of the images of both modalities obtained simultaneously in a single session (14). Several studies have shown that increased ^{18}F-FDG uptake in carotid artery plaques can qualify the degree of vascular inflammation (11,15). Others using PET/CT have reported uptake of ^{18}F-FDG in diseased thoracic aortas of patients with AAD (16,17). However, the pathology and clinical implications of the ^{18}F-FDG PET/CT findings remain to be elucidated.

The aims of this prospective study were to compare ^{18}F-FDG uptake in the thoracic aorta between AAD patients and healthy controls and to assess the clinical significance of ^{18}F-FDG uptake on PET/CT images for predicting short- and midterm outcomes in medically controlled AAD patients.

MATERIALS AND METHODS

Population and Protocol

This study enrolled 28 patients with AAD (17 men and 11 women; mean age $\pm$ SD, 69.5 $\pm$ 11.6 y) who had an emergency admission to our hospital between April 2006 and November 2008. The patients included those with Stanford type B AAD ($n = 26$) treated by medical therapy and those with Stanford type A AAD ($n = 2$) who could not undergo surgical repair because of severe comorbidity and advanced age. All patients were examined initially by chest radiography, laboratory tests for serum myocardial marker and D-dimer, electrocardiography, and echocardiography followed by contrast medium–enhanced CT. Aortic dissection was defined as a separation of the aortic wall layers, with resulting true and false lumens, or as intramural hematoma examined by enhanced chest CT (4). Individuals with chronic renal disease (serum creatinine level > 2.0 mg/dL), poorly treated diabetes, Marfan syndrome, Ehlers-Danlos syndrome, a traumatic aneurysm, a bicuspid aortic valve, arteritis, a pseudoaneurysm, a mycotic aneurysm, a connective tissue disorder, or congenital malformations of the heart or vessels were excluded from the study.

Blood samples were taken for lipid profiles, glycosylated hemoglobin A1c, D-dimer, high-sensitivity C-reactive protein, and matrix metalloproteinases 2 (MMP-2) and 9 (MMP-9). D-dimer was measured by latex agglutination. High-sensitivity C-reactive protein was measured by particle-enhanced immunonephelometry. MMP-2 and -9 were determined by the sensitive 2-step sandwich enzyme immunoassay system using 2 monoclonal antibodies against them.

An unfavorable outcome was defined as death from cardiovascular causes, rupture or progression of the aortic dissection, conversion to surgical repair, and cardiovascular events during or after the initial hospitalization. The follow-up periods for assessing short- and midterm outcomes were defined as 1 mo after the onset of AAD (including the acute hospital stay) and 6 mo after the onset, respectively. All patients were followed up by a physician's examination and enhanced chest CT according to the usual standard of care with antihypertensive therapy. Fourteen age- and sex-matched individuals (7 men and 7 women) who visited outpatient clinics of our hospitals for cancer screening and did not have a history of malignant, inflammatory, cardiovascular, cerebrovascular, or aortic disease served as controls for the evaluation of PET/CT images.

The study protocol complied with the Declaration of Helsinki and was approved by the Committee on the Ethics of Human Research of Gifu Prefectural Tajimi Hospital. Each patient gave written informed consent.

Enhanced CT

A series of CT examinations was performed to evaluate progression, rupture, and the following morphologic parameters: maximum aortic dissection diameter; diameter of false and true lumen; reference aortic diameter; and the presence of intramural hematoma, penetrating atherosclerotic ulcer, thrombosed false lumen, and true lumen compression. A continuous-spiral 64-detector scanner was used (Aquilion 64; Toshiba Medical Systems), with a tube voltage of 120 kV, helical pitch of 21.0, slice thickness of 1.2 mm, and rotation speed of 0.5 s/revolution. The examinations were performed at 1 wk, 1 mo, 3 mo, 6 mo, and 1 y after the onset of AAD, before and during intravenous injection of contrast agent (370 mg of iodine/mL, 1.5 mL/kg of body weight) The radiation burden to the patient was 30 mAs in each CT acquisition. An intramural hematoma was defined as a more than 5-mm semicircular or circular thickening of the aortic wall without intimal disruption; penetrating aortic ulcer was defined as a craterlike ulceration in the aortic wall with or without adjacent subintimal hematoma.

^{18}F-FDG PET/CT

According to routine protocol, unenhanced CT and PET images were acquired consecutively 50 and 100 min after the injection of 4–6 MBq of ^{18}F-FDG per kilogram, using a PET/CT system (Biograph 6; Siemens Medical Solutions) combining a multislice spiral CT scanner with a full-ring PET scanner with lutetium oxyorthosilicate crystals. The patients underwent scanning at 12.2 $\pm$ 5.3 d after their admission. The interval between the onset of AAD and ^{18}F-FDG PET/CT scanning was 13.2 $\pm$ 6.1 d, and 6 patients had a late diagnosis of AAD. The CT acquisition parameters were as follows: 130 kV, 30 mA, 6 helical slices, 0.5 s/rotation, a pitch of 1.5, and a slice thickness of 5 mm. The PET images were acquired sequentially over an 80-cm field of view during 10 min in 3-dimensional mode. Matching PET and CT slices were fused, and an image of the ^{18}F-FDG activity overlying the corresponding anatomic plane was reconstructed using iterative ordered-subset expectation maximization on a dedicated workstation (e.softTurbo-V WorkStation SMS; Siemens Medical Solutions).

Image Interpretation

Noncorrected and attenuation-corrected PET images, CT images, and PET/CT images were available for review, displayed in axial, coronal, and sagittal planes. Using the corresponding PET/CT images, 3 radiologists working in consensus and not aware of the clinical data determined the location of abnormal focal ^{18}F-FDG uptake in relation to the vascular wall and dissection on enhanced CT images. In all examinations for both patients and

controls, 5-mm circular regions of interest were drawn at 3 different sites on the aortic dissection or normal aorta: the most proximal site; the site with maximal dissection (or, for normal aortas, a site intermediary between most proximal and most distal); and the most distal site. Areas with maximal focal ^{18}F-FDG uptake were visually detected, and the maximal standardized uptake value (SUV_{max}) and mean standardized uptake value (SUV_{mean}) in each area were measured by computational analysis software (VOX-BASE Browser/View; J-Mac system).

Data Analysis

Continuous variables are expressed as mean ± SD, unless otherwise stated, and were compared using either the unpaired Student t test, the Mann–Whitney test if data did not show a normal distribution, or ANOVA followed by the multiple-comparison test with Bonferroni adjustment. Categoric variables, expressed as percentages, were compared using the χ^2 test or Fisher exact test. Significant univariate risk factors were followed by application of multivariate analysis. The receiver-operating-characteristic curve was estimated to assess the predictive power of ^{18}F-FDG SUV, with calculation of the area under these curves. Statistical significance was examined by 2-sided tests. A P value of less than 0.05 was considered statistically significant.

RESULTS

Table 1 shows the demographic data for the AAD patients. The mean observation period and hospital stay were 6.4 ± 5.4 mo (range, 21.3–0.3 mo) and 21.5 ± 10.8 d, respectively. During the initial hospitalization, no patients died; however, life-threatening morbidities such as stroke ($n = 1$), cardiac tamponade ($n = 2$), pleural effusion ($n = 13$), shock ($n = 1$), acute renal failure ($n = 6$), mesenteric ischemia ($n = 1$), and limb ischemia ($n = 2$) were observed as complications of AAD. Of the 28 patients, 8 were classified as having unfavorable AAD: 2 who had an unfavorable outcome because of death from dissection rupture during follow-up, 4 who had surgical repair associated with progression of dissection during ($n = 2$) or after ($n = 2$) the initial hospital stay, and 2 who had progression of dissection during follow-up. The remaining 20 patients were classified as having favorable AAD: the dissection almost entirely disappeared in 6, the dissection regressed in 6, and the size and morphology of the dissection showed no remarkable change in the other 8. No significant difference was observed between the favorable and unfavorable AAD groups except for the presence of chest pain ($P = 0.0296$), radiating pain ($P = 0.0200$), and any pulse deficit ($P = 0.0351$), as shown in Table 1. No adverse events related to medication occurred during the hospitalization.

Table 2 shows CT data and levels of measured biomarkers in the 2 groups. Maximum dissection diameter and mean value of high-density lipoprotein (HDL) cholesterol were significantly different between the favorable and unfavorable AAD groups ($P = 0.0207$, $P = 0.0135$, respectively).

Table 3 presents data for the accumulation of ^{18}F-FDG in controls, favorable AAD patients, and unfavorable AAD

patients at the 3 different sites for 50-min images. The ^{18}F-FDG SUV_{max} and SUV_{mean} of both AAD groups were significantly greater than those of controls at both the proximal and the distal sites. The ^{18}F-FDG SUV_{max} and SUV_{mean} of the unfavorable AAD group were significantly greater than those of the favorable group at the site of maximum aortic dissection. Concerning the analysis of ^{18}F-FDG uptake on 100-min images, despite a significantly higher ^{18}F-FDG SUV_{max} and SUV_{mean} in both AAD groups than in controls at the 3 sites (all $P < 0.05$), no significant difference in either ^{18}F-FDG SUV_{max} or SUV_{mean} at the 3 sites was observed between the favorable and unfavorable AAD groups. The total volume of ^{18}F-FDG injected for each study was 233.0 ± 39.9 MBq.

Additionally, a stepwise-forward selection procedure with adjustment for covariates, including clinical presentation, HDL cholesterol, and maximum dissection diameter, demonstrated that the ^{18}F-FDG SUV_{mean} of 50-min images at the site of maximum aortic dissection significantly and independently predicted an unfavorable outcome of AAD ($P = 0.0171$; odds ratio, 7.72; 95% confidence interval, 1.44–41.4; $R^2 = 0.2372$).

Analysis of the area under the curve for 50-min images was used to assess the predictive accuracy of ^{18}F-FDG SUV_{mean} at the site of maximum aortic dissection for short- and midterm outcomes of AAD (Fig. 1). The mean area under the curve for SUV_{mean} (±SE of mean) was 0.79375 ± 0.08893. For the prediction of unfavorable outcome, the optimal SUV_{mean} cutoff level determined from the receiver-operating-characteristic curves was 3.029. This level demonstrated a sensitivity of 75.0%, specificity of 70.0%, positive predictive value of 50.0%, negative predictive value of 87.5%, accuracy of 71.4%, and odds ratio of 4.00.

In subgroup analysis, the favorable AAD group was divided into 2 categories: an improved AAD subgroup consisting of patients whose AAD disappeared ($n = 6$) or regressed ($n = 6$) and a stable AAD subgroup consisting of patients whose dissection showed no remarkable change ($n = 8$). Significant incremental changes in ^{18}F-FDG SUV_{max} and SUV_{mean} on 50-min images were observed at the site of maximum aortic dissection between controls, improved AAD patients, stable AAD patients, and unfavorable AAD patients ($P < 0.0001$ [ANOVA]; Table 4).

Figure 1 shows 2 representative patients. An 82-y-old woman with a favorable outcome for type B AAD showed less ^{18}F-FDG uptake on PET/CT, consistent with the intramural hematoma on contrast-enhanced CT. This patient experienced AAD regression at 2 mo after onset. In contrast, a 44-y-old man with an unfavorable AAD outcome showed greater ^{18}F-FDG uptake on PET/CT, consistent with the dissected aortic wall on contrast-enhanced CT. This patient electively underwent aortic aneurysm repair because of AAD progression at 3 mo after onset. Interestingly, ^{18}F-FDG uptake at the flap that separated the aortic wall layers was observed in this patient.

TABLE 1. Baseline Characteristics of Study Subjects

Characteristic	Favorable AAD ($n = 20$)	Unfavorable AAD ($n = 8$)	P^*
Age (y)	68.1 ± 11.8	73.1 ± 11.2	0.2849
Female	8 (40.0%)	3 (37.5%)	0.9026
Body mass index (kg/m^2)	24.0 ± 4.4	24.0 ± 4.0	0.5977
Stanford A	1 (5%)	1 (12.5%)	0.5067
Past medical history			
Hypertension	16 (80.0)	7 (87.5)	0.6301
Dyslipidemia	4 (20.0)	3 (37.5)	0.3340
Diabetes mellitus	2 (10.0)	0 (0.0)	0.3533
Coronary artery disease	3 (15.0)	3 (37.5)	0.1899
Cardiac surgery	1 (5)	1 (12.5)	0.5067
Chronic obstructive pulmonary disease	4 (20.0)	2 (25.0)	0.7733
Familial history	0 (0)	0 (0)	—
Clinical presentation			
Chest pain	3 (15.0)	5 (62.5)	0.0296[†]
Back pain	15 (75.0)	3 (37.5)	0.0644
Migrating pain	7 (35.0)	4 (50.0)	0.5805
Radiating pain	0 (0.0)	2 (25.0)	0.0200[†]
Any pulse deficit	1 (5.0)	3 (37.5)	0.0351[†]
Neurologic deficit	0 (0.0)	0 (0.0)	—
Hypotension and shock	1 (5.0)	0 (0.0)	0.5195
Hypertension	11 (55.0)	5 (62.5)	0.7171
Complications			
Cardiac tamponade	1 (5)	1 (12.5)	0.5067
Aortic valve regurgitation	2 (10.0)	1 (12.5)	0.8488
Congestive heart failure	1 (5.0)	2 (25.0)	0.1222
Stroke	1 (5.0)	0 (0.0)	0.5195
Acute renal failure	3 (15.0)	3 (37.5)	0.1899
Mesenteric ischemia	1 (5.0)	0 (0.0)	0.5195
Limb ischemia	1 (5)	1 (12.5)	0.5067
Chest radiography findings			
Abnormal cardiac contour	17 (85.0)	7 (87.5)	0.8629
Widened mediastinum	17 (85.0)	6 (75.0)	0.5427
Pleural effusion	8 (40.0)	5 (62.5)	0.2799
Electrocardiography findings			
Left ventricular hypertrophy	5 (25.0)	3 (37.5)	0.5146
ST elevation	5 (25.0)	3 (37.5)	0.5146
ST depression	4 (20.0)	1 (12.5)	0.6301
Abnormal T or Q wave	8 (40.0)	4 (50.0)	0.6300
Length of hospital stay (d)	19.0 ± 8.3	27.8 ± 14.1	0.1466
Mean time to endpoints (mo)	6.8 ± 5.4	5.4 ± 5.7	0.2742
Range of times to endpoints (mo)	21.8–1.3	16.3–0.3	
Initial medication			0.6899
β-blocker	14 (70.0)	7 (87.5)	
Calcium channel blocker	15 (75.0)	3 (37.5)	
Angiotensin-converting enzyme inhibitor or angiotensin receptor blocker	17 (85.0)	6 (75.0)	
Statins	10 (50.0)	3 (37.5)	

*For differences between favorable and unfavorable AAD groups.

[†]$P < 0.05$.

Unless otherwise indicated, data are presented as *n,* with percentage in parentheses, or as mean ± SD.

DISCUSSION

The present study yielded the following results: ^{18}F-FDG SUV was significantly greater in AAD patients than in controls. When unfavorable and favorable AAD patients were compared, ^{18}F-FDG SUV at the site of maximum aortic dissection was significantly greater in unfavorable than in favorable AAD patients. Multivariate analysis showed that ^{18}F-FDG SUV$_{mean}$ at the site of maximum aortic dissection independently predicted an unfavorable outcome for AAD. An SUV$_{mean}$ cutoff of 3.029 demonstrated reliable predictive powers.

The pathologic features of AAD include degeneration of the medial elastic fibers, thinning of the media, loss of smooth muscle cells, adventitial hypertrophy, and accumulation of lymphocytes and macrophages secreting several kinds of enzymes, particularly MMPs, that have been

TABLE 2. Data from Chest CT and Laboratory Tests in Patients with AAD

Characteristic	Favorable AAD ($n = 20$)	Unfavorable AAD ($n = 8$)	$P*$
Chest CT findings			
Intramural hematoma	14 (70.0)	6 (75.0)	0.7897
True lumen compression	3 (15.0)	3 (37.5)	0.2055
Thrombosed false lumen	15 (75.0)	6 (75.0)	1.0000
Penetrating atherosclerotic ulcer	9 (45.0)	5 (62.5)	0.4009
True lumen diameter (mm)	23.9 ± 6.3	24.9 ± 4.5	0.5223
False lumen diameter (mm)	13.9 ± 6.2	11.8 ± 1.3	0.8035
False-to-true lumen ratio (mm)	0.68 ± 0.34	0.49 ± 0.13	0.4807
Maximum dissection diameter (mm)	40.0 ± 8.9	46.5 ± 4.7	0.0207†
Reference aortic diameter (mm)	32.7 ± 3.7	36.1 ± 6.2	0.2128
Laboratory tests			
Low-density-lipoprotein cholesterol (mg/dL)	119.0 ± 40.8	119.0 ± 38.9	0.8587
Triglyceride (mg/dL)	109.4 ± 65.0	92.0 ± 24.3	0.8388
HDL cholesterol (mg/dL)	47.9 ± 15.6	33.4 ± 7.8	0.0135†
Glycosylated hemoglobin A1c (%)	5.4 ± 0.6	5.5 ± 0.4	0.7401
Serum creatine level (mg/dL)	0.82 ± 0.29	0.82 ± 0.38	0.6466
D-dimer (μg/mL)	8.0 ± 8.5	11.0 ± 12.5	0.5931
High-sensitivity C-reactive protein (ng/mL)	42,674.9 ± 47,551.1	52,386.0 ± 56,662.6	0.7029
MMP-2 (ng/mL)	702.4 ± 160.2	771.0 ± 288.5	0.8034
MMP-9 (ng/mL)	92.0 ± 72.8	57.3 ± 55.4	0.0709

*For differences between favorable and unfavorable AAD groups.
†$P < 0.05$.
Unless otherwise indicated, data are presented as *n,* with percentage in parentheses, or as mean ± SD.

implicated in medial degradation (*18–20*). A previous study showed that small numbers of macrophages surrounding areas of cystic medial necrosis were immunopositive for several MMPs, including MMP-2 and -9, that can degrade elastin (*21*). Thus, macrophages are the predominant leukocyte that initiates aneurysm formation by producing inflammatory cytokines and proteolytic enzymes (*22*).

Several studies reported that increased uptake of ^{18}F-FDG in the atherosclerotic vascular wall correlated with dense infiltrations of macrophages and the number of macrophages in the plaque (*11,16,23*). These results support the idea that uptake of ^{18}F-FDG may depict and qualify macrophage content as a marker of atherosclerotic inflammation within the aortic wall. Some studies demonstrated a relationship between the degree of inflammation and vascular complications or outcome of AAD (*24,25*). A greater serum CRP elevation at admission in patients with type B AAD was significantly associated with a poorer clinical outcome. Hence, it seems plausible that increased ^{18}F-FDG accumulation in an aortic dissection stems from macrophage density indicating inflammation in the aortic wall and thus could be correlated with short- and midterm outcomes for AAD.

In the present study, only 50-min images demonstrated a significant association between ^{18}F-FDG SUV at the site of maximum aortic dissection and short- and midterm

TABLE 3. Accumulation of ^{18}F-FDG in Aortic Wall in Controls, Favorable AAD Patients, and Unfavorable AAD Patients on 50-Minute Images

| Site	Controls ($n = 14$)	Favorable AAD ($n = 20$) Data	*P* vs. controls	Unfavorable AAD ($n = 8$) Data	*P* vs. controls	*P* vs. favorable AAD	*P* (ANOVA)
Proximal							
SUV_{max}	2.31 ± 0.29	3.91 ± 1.00	0.0001*	4.33 ± 1.63	0.0001*	0.932	<0.0001*
SUV_{mean}	1.84 ± 0.23	3.03 ± 0.83	0.0001*	3.18 ± 1.07	0.0007*	1.0000	<0.0001*
Maximum							
SUV_{max}	2.34 ± 0.32	3.10 ± 1.18	0.1310	4.52 ± 1.44	<0.0001*	0.0069*	0.0001*
SUV_{mean}	1.85 ± 0.18	2.36 ± 0.93	0.1680	3.44 ± 0.87	<0.0001*	0.0043*	0.0001*
Distal							
SUV_{max}	2.59 ± 0.34	3.64 ± 0.96	0.0018*	3.84 ± 0.96	0.0036*	1.0000	0.0007*
SUV_{mean}	2.00 ± 0.21	2.71 ± 0.67	0.0024*	2.86 ± 0.66	0.0039*	1.0000	0.0008*

*$P < 0.05$.
Data are presented as mean ± SD.
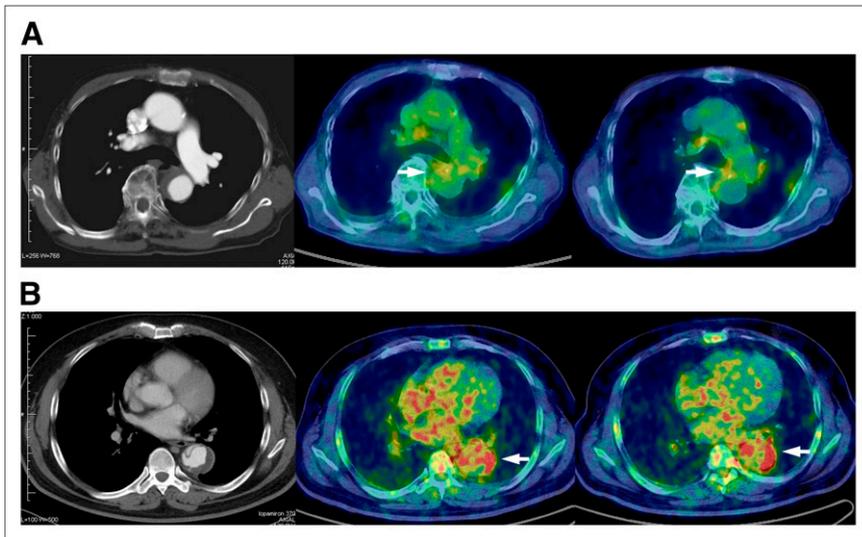
FIGURE 1. (A) Patient with favorable AAD outcome. Enhanced CT (left) shows type B AAD consistent with low uptake of ^{18}F-FDG in intramural hematoma lesion on transaxial PET/CT at 50 min (middle) and 100 min (right). This 82-y-old woman experienced AAD regression 2 mo after onset. ^{18}F-FDG SUV$_{max}$ and SUV$_{mean}$ were 3.068 and 2.447, respectively, on 50-min images and 2.740 and 2.309, respectively, on 100-min images. (B) Patient with unfavorable AAD outcome. Enhanced CT (left) shows type B AAD consistent with high uptake of ^{18}F-FDG in dissected aortic wall on transaxial PET/CT at 50 min (middle) and 100 min (right). This 44-y-old man underwent elective repair of aortic aneurysm because of AAD progression 3 mo after onset. ^{18}F-FDG SUV$_{max}$ and SUV$_{mean}$ were 6.785 and 5.254, respectively, on 50-min images and 8.16 and 5.956, respectively, on 100-min images. ROIs are indicated by arrows.

outcomes for AAD. ^{18}F-FDG uptake by inflammatory cells peaked at approximately 60 min after injection and then decreased gradually (*26*). Glucose-6-phosphatase mediates the dephosphorylation of intracellular ^{18}F-FDG. Unless ^{18}F-FDG-6-phosphate is dephosphorylated by glucose-6-phosphatase, it is unable to leave the cell. Macrophages have high levels of glucose-6-phosphatase and a relatively low ratio of hexokinase to phosphatase (*26*). Consequently, in macrophages, ^{18}F-FDG-6-phosphate can be rapidly dephosphorylated and cleared after reaching a certain level. The interval between tracer injection and scanning is likely to be a factor that may affect the difference in our results between 50- and 100-min images.

Kuehl et al. found that one third of 33 patients with acute aortic syndrome had ^{18}F-FDG uptake indicating active vessel wall inflammation (*16*). There was a trend toward an association between greater uptake of ^{18}F-FDG and poorer outcome. However, in the study by Kuehl et al., if an ^{18}F-FDG SUV$_{mean}$ of more than 2.5 was positive, positive PET/CT findings did not significantly correlate with the clinical outcome of patients with acute aortic syndrome including aortic aneurysm and dissection (*16*). In the present study, in which patients with aortic aneurysm were excluded, given the SUV$_{mean}$ cutoff value of 3.029, ^{18}F-FDG PET had a substantial predictive value for discriminating unfavorable from favorable AAD patients. The difference between the results of Kuehl et al. and our results is possibly attributable to the presence or absence of an aortic aneurysm in the studied patients. Reportedly, macrophages were present in the aortic media in both aortic dissection patients and aneurysm patients; however, greater numbers of macrophages were noted in the aortas of

TABLE 4. Subgroup Analysis of ^{18}F-FDG Uptake in Aortic Wall in Controls and in Patients with Improved, Stable, or Unfavorable AAD on 50-Minute Images

Site	Controls (*n* = 14)	Improved AAD (*n* = 12)	Stable AAD (*n* = 8)	Unfavorable AAD (*n* = 8)	P (ANOVA)
Proximal					
SUV$_{max}$	2.31 ± 0.29	3.89 ± 1.16*	3.92 ± 0.78*	4.33 ± 1.63*	<0.0001†
SUV$_{mean}$	1.84 ± 0.23	3.02 ± 0.97*	3.06 ± 0.62*	3.18 ± 1.07*	0.0002†
Maximum					
SUV$_{max}$	2.34 ± 0.32	2.77 ± 1.22	3.59 ± 0.99	4.52 ± 1.44*‡	0.0001†
SUV$_{mean}$	1.85 ± 0.18	2.11 ± 0.97	2.74 ± 0.75	3.44 ± 0.87*‡	<0.0001†
Distal					
SUV$_{max}$	2.59 ± 0.34	3.76 ± 0.93*	3.46 ± 1.05	3.84 ± 0.96*	0.0018†
SUV$_{mean}$	2.00 ± 0.21	2.73 ± 0.63*	2.67 ± 0.76	2.86 ± 0.66*	0.0028†

*$P < 0.05$ vs. controls.
†$P < 0.05$.
‡$P < 0.05$ vs. improved AAD.
Data are presented as mean ± SD.

patients who had aortic dissections (20). This finding may account for the difference in uptake of ^{18}F-FDG between aortic aneurysms and dissections.

Besides the classically known determinants of AAD prognosis, that is, aneurysm diameter, the female sex, older age, cardiac tamponade, partial thrombosis of a false lumen, renal failure, and hypotension or shock (27,28), identification of an aortic dissection at high risk of rupture and progression is an ultimate goal for noninvasive vascular inflammatory imaging. Our observation that, on metabolic imaging for vascular inflammation, ^{18}F-FDG uptake with trapping is directly proportional to AAD outcome suggests the usefulness of ^{18}F-FDG PET/CT for risk stratification among AAD patients.

In the present study, almost the entire dissection disappeared in 6 patients (30%), and the dissection regressed in another 6 (30%) among the favorable AAD group (n = 20). Although it remains inconclusive whether this is the clinical nature of AAD, Kaji et al. reported that of 22 consecutive patients with AAD, 6 (27%) showed regression of AAD at follow-up, and another 6 (27%) showed disappearance of AAD (29). Other studies also reported disappearance and regression of AAD at follow-up, consistent with our results (30,31). With CT alone, it is difficult to detect pathologic changes in the dissected aorta and to clarify the pathologic mechanism of the disappearance or regression of AAD (29). Other imaging modalities, such as PET/CT, may be able to detect pathologic changes in these conditions though follow-up with serial PET/CT.

Interestingly, the present study demonstrated that HDL cholesterol levels were significantly higher in favorable than unfavorable AAD patients. HDL cholesterol has antioxidant and antiinflammatory effects that may contribute to its antiatherogenic potential (32). Thus, the difference in outcome of AAD patients is potentially, at least in part, attributable to these effects of HDL cholesterol and a difference in HDL cholesterol levels between favorable and unfavorable AAD patients.

Like other observational studies, this study had several potential limitations that may affect the data analysis. As there were no good prior data, sample size could not be estimated correctly. Even though this was a prospective study of consecutive patients, the period over which data were collected was arbitrarily selected. The possibility exists that respiratory motion or our use of CT attenuation correction may have led to a false-positive result. ^{18}F-FDG uptake findings in aortic dissection were not compared with histopathologic findings. It is not possible to differentiate causative factors and epiphenomena on the basis of ^{18}F-FDG PET/CT findings.

CONCLUSION

Greater uptake of ^{18}F-FDG in the dissected aortic wall was significantly associated with an increased risk for rupture and progression of aortic dissection and thus could discriminate favorable from unfavorable AAD patients. Stratification of AAD patients by evaluating ^{18}F-FDG uptake may therefore be important in predicting short- and midterm outcomes and thereby achieving effective management.

REFERENCES

1. Chiesa R, Melissano G, Civilini E, de Moura ML, Carozzo A, Zangrillo A. Ten years experience of thoracic and thoracoabdominal aortic aneurysm surgical repair: lessons learned. *Ann Vasc Surg.* 2004;18:514–520.
2. Nienaber CA, Eagle KA. Aortic dissection: new frontiers in diagnosis and management: Part I: from etiology to diagnostic strategies. *Circulation.* 2003; 108:628–635.
3. Suzuki T, Mehta RH, Ince H, et al. Clinical profiles and outcomes of acute type B aortic dissection in the current era: lessons from the International Registry of Aortic Dissection (IRAD). *Circulation.* 2003;108(suppl 1): II312–II317.
4. Olsson C, Thelin S, Stahle E, Ekbom A, Granath F. Thoracic aortic aneurysm and dissection: increasing prevalence and improved outcomes reported in a nationwide population-based study of more than 14,000 cases from 1987 to 2002. *Circulation.* 2006;114:2611–2618.
5. Song JM, Kim SD, Kim JH, et al. Long-term predictors of descending aorta aneurysmal change in patients with aortic dissection. *J Am Coll Cardiol.* 2007; 50:799–804.
6. Reeps C, Essler M, Pelisek J, Seidl S, Eckstein HH, Krause BJ. Increased ^{18}F-fluorodeoxyglucose uptake in abdominal aortic aneurysms in positron emission/computed tomography is associated with inflammation, aortic wall instability, and acute symptoms. *J Vasc Surg.* 2008;48:417–423.
7. Daily PO, Trueblood HW, Stinson EB, Wuerflein RD, Shumway NE. Management of acute aortic dissections. *Ann Thorac Surg.* 1970;10:237–247.
8. Barbour JR, Spinale FG, Ikonomidis JS. Proteinase systems and thoracic aortic aneurysm progression. *J Surg Res.* 2007;139:292–307.
9. Guo DC, Papke CL, He R, Milewicz DM. Pathogenesis of thoracic and abdominal aortic aneurysms. *Ann N Y Acad Sci.* 2006;1085:339–352.
10. Tahara N, Kai H, Yamagishi S, et al. Vascular inflammation evaluated by [^{18}F]-fluorodeoxyglucose positron emission tomography is associated with the metabolic syndrome. *J Am Coll Cardiol.* 2007;49:1533–1539.
11. Rudd JH, Warburton EA, Fryer TD, et al. Imaging atherosclerotic plaque inflammation with [^{18}F]-fluorodeoxyglucose positron emission tomography. *Circulation.* 2002;105:2708–2711.
12. Dunphy MP, Freiman A, Larson SM, Strauss HW. Association of vascular ^{18}F-FDG uptake with vascular calcification. *J Nucl Med.* 2005;46:1278–1284.
13. Ogawa M, Ishino S, Mukai T, et al. ^{18}F-FDG accumulation in atherosclerotic plaques: immunohistochemical and PET imaging study. *J Nucl Med.* 2004; 45:1245–1250.
14. Bar-Shalom R, Yefremov N, Guralnik L, et al. Clinical performance of PET/CT in evaluation of cancer: additional value for diagnostic imaging and patient management. *J Nucl Med.* 2003;44:1200–1209.
15. Tahara N, Kai H, Ishibashi M, et al. Simvastatin attenuates plaque inflammation: evaluation by fluorodeoxyglucose positron emission tomography. *J Am Coll Cardiol.* 2006;48:1825–1831.
16. Kuehl H, Eggebrecht H, Boes T, et al. Detection of inflammation in patients with acute aortic syndrome: comparison of FDG-PET/CT imaging and serological markers of inflammation. *Heart.* 2008;94:1472–1477.

17. Ryan A, McCook B, Sholosh B, et al. Acute intramural hematoma of the aorta as a cause of positive fluorodeoxyglucose positron emission tomography/computed tomography. *J Thorac Cardiovasc Surg.* 2007;134:520–521.

18. Lopez-Candales A, Holmes DR, Liao S, Scott MJ, Wickline SA, Thompson RW. Decreased vascular smooth muscle cell density in medial degeneration of human abdominal aortic aneurysms. *Am J Pathol.* 1997;150:993–1007.

19. Gong Y, Hart E, Shchurin A, Hoover-Plow J. Inflammatory macrophage migration requires MMP-9 activation by plasminogen in mice. *J Clin Invest.* 2008;118:3012–3024.

20. He R, Guo DC, Estrera AL, et al. Characterization of the inflammatory and apoptotic cells in the aortas of patients with ascending thoracic aortic aneurysms and dissections. *J Thorac Cardiovasc Surg.* 2006;131:671–678.

21. Segura AM, Luna RE, Horiba K, et al. Immunohistochemistry of matrix metalloproteinases and their inhibitors in thoracic aortic aneurysms and aortic valves of patients with Marfan's syndrome. *Circulation.* 1998;98(19 suppl): II331–II337.

22. Shimizu K, Mitchell RN, Libby P. Inflammation and cellular immune responses in abdominal aortic aneurysms. *Arterioscler Thromb Vasc Biol.* 2006;26:987–994.

23. Vallabhajosula S, Fuster V. Atherosclerosis: imaging techniques and the evolving role of nuclear medicine. *J Nucl Med.* 1997;38:1788–1796.

24. Schillinger M, Domanovits H, Bayegan K, et al. C-reactive protein and mortality in patients with acute aortic disease. *Intensive Care Med.* 2002;28:740–745.

25. Sugano Y, Anzai T, Yoshikawa T, et al. Serum C-reactive protein elevation predicts poor clinical outcome in patients with distal type acute aortic dissection: association with the occurrence of oxygenation impairment. *Int J Cardiol.* 2005; 102:39–45.

26. Zhuang H, Pourdehnad M, Lambright ES, et al. Dual time point ^{18}F-FDG PET imaging for differentiating malignant from inflammatory processes. *J Nucl Med.* 2001;42:1412–1417.

27. Tsai TT, Evangelista A, Nienaber CA, et al. Partial thrombosis of the false lumen in patients with acute type B aortic dissection. *N Engl J Med.* 2007;357:349–359.

28. Tsai TT, Fattori R, Trimarchi S, et al. Long-term survival in patients presenting with type B acute aortic dissection: insights from the International Registry of Acute Aortic Dissection. *Circulation.* 2006;114:2226–2231.

29. Kaji S, Nishigami K, Akasaka T, et al. Prediction of progression or regression of type A aortic intramural hematoma by computed tomography. *Circulation.* 1999;100(19, suppl)II281–II286.

30. Kaji S, Akasaka T, Horibata Y, et al. Long-term prognosis of patients with type A aortic intramural hematoma. *Circulation.* 2002;106(12, suppl 1)I248–I252.

31. Nishigami K, Tsuchiya T, Shono H, Horibata Y, Honda T. Disappearance of aortic intramural hematoma and its significance to the prognosis. *Circulation.* 2000;102(19, suppl 3)III243–III247.

32. Barter PJ, Nicholls S, Rye KA, Anantharamaiah GM, Navab M, Fogelman AM. Antiinflammatory properties of HDL. *Circ Res.* 2004;95:764–772.